⌘ *Author's Choice*

THE JOURNAL OF BIOLOGICAL CHEMISTRY VOL. 290, NO. 12, pp. 7973–7979, March 20, 2015
© 2015 by The American Society for Biochemistry and Molecular Biology, Inc. Published in the U.S.A.

DNA Induces Conformational Changes in a Recombinant Human Minichromosome Maintenance Complex*

Received for publication, October 30, 2014, and in revised form, February 2, 2015 Published, JBC Papers in Press, February 3, 2015, DOI 10.1074/jbc.M114.622738

Emma L. Hesketh[‡1,2], **Richard P. Parker-Manuel**[‡1,3], **Yuriy Chaban**[§4], **Rabab Satti**[‡5], **Dawn Coverley**[‡], **Elena V. Orlova**[§], **and James P. J. Chong**[‡6]

From the [‡]*Department of Biology, University of York, York YO10 5DD and the* [§]*Department of Crystallography, Birkbeck College London, London WC1E 7HX, United Kingdom*

Background: The human minichromosome maintenance (hMCM) complex is an important component of the DNA replication apparatus.
Results: After being produced in *Escherichia coli*, hMCM has ATPase and DNA helicase activity and undergoes a conformational change when bound to DNA.
Conclusion: Recombinant hMCM is functional *in vitro*.
Significance: hMCM provides an important tool for the biochemical reconstitution of the human replicative helicase.

ATP-dependent DNA unwinding activity has been demonstrated for recombinant archaeal homohexameric minichromosome maintenance (MCM) complexes and their yeast heterohexameric counterparts, but in higher eukaryotes such as *Drosophila*, MCM-associated DNA helicase activity has been observed only in the context of a co-purified Cdc45-MCM-GINS complex. Here, we describe the production of the recombinant human MCM (hMCM) complex in *Escherichia coli*. This protein displays ATP hydrolysis activity and is capable of unwinding duplex DNA. Using single-particle asymmetric EM reconstruction, we demonstrate that recombinant hMCM forms a hexamer that undergoes a conformational change when bound to DNA. Recombinant hMCM produced without post-translational modifications is functional *in vitro* and provides an important tool for biochemical reconstitution of the human replicative helicase.

DNA replication is fundamental to the proliferation of all cells and, as such, has been the subject of intense scrutiny over many years. Although this work has demonstrated many unifying similarities among all eukaryotes with regard to DNA replication, it has also become obvious that there are a number of differences in the details regarding these systems. Significantly, one of the main model organisms for eukaryotic DNA replication, the yeast *Saccharomyces cerevisiae*, has a closed mitosis that requires replication proteins to cross the nuclear envelope in a manner not required in other eukaryotes (1). The minichromosome maintenance (MCM)[7] proteins are a good example of such proteins, and *S. cerevisiae* MCM proteins possess insertions to cater to this requirement (Table 1). The models used to study replication in *Xenopus* and *Drosophila* are egg-based and contain unusually high levels of (likely preassembled) replication complexes not normally seen in post-embryonic systems (2). Data from human tissue culture studies are based mainly on transformed cells, which probably do not accurately reflect the cell cycle controls in primary explants (3). Thus, the use of recombinant components, which may more accurately reconstitute robust DNA helicase activity biochemically, is of significant interest in understanding human DNA replication processes.

The MCM complex is essential for DNA replication in eukaryotes and archaea, where it is believed to act as the replicative DNA helicase (reviewed in Ref. 4). Homohexameric archaeal MCM complexes have provided useful models for studying DNA helicase activity (5, 6). The production of a number of crystal structures has facilitated mapping of key enzyme residues and provided insight into the molecular mechanisms utilized in DNA unwinding and translocation (7, 8). In addition to its essential role in DNA replication, the heterohexameric eukaryotic MCM2–7 complex has been implicated in DNA damage responses, checkpoint signaling, transcription, and chromatin remodeling (9–12).

Isolation of intact functional MCM heterohexamers has proved challenging. Functional MCM complexes purified from *Xenopus* egg extracts using a replication licensing factor assay demonstrated an additional requirement for Cdt1 in MCM chromatin loading (13, 14). A Cdc45-MCM-GINS complex with DNA helicase activity has been isolated from *Drosophila* egg extracts (15). MCM function is post-transla-

* This work was supported by Cancer Research UK Grants A7771 and A10945; Wellcome VIP funds administered by the Department of Biology, University of York; and Yorkshire Cancer Research Grant Y002PhD.
⌘ *Author's Choice*—Final version full access.
The electron density maps have been deposited in the EMDataBank (codes EMDB-2872 and EMDB-2873).
[1] Both authors contributed equally to this work.
[2] Present address: Astbury Centre for Structural Molecular Biology, University of Leeds, Leeds LS2 9JT, United Kingdom.
[3] Present address: Inst. of Parasitology, Justus-Liebig-University Giessen, 35392 Giessen, Germany.
[4] Present address: Institute of Cancer Research, London SW7 3RP, United Kingdom.
[5] Present address: Dept. of Biochemistry, Faculty of Biological Sciences, Quaid-i-Azam University, Islamabad 45320, Pakistan.
[6] To whom correspondence should be addressed: Dept. of Biology, University of York, York YO10 5DD, United Kingdom. Tel.: 44-1904-328628; Fax: 44-1904-328505; E-mail: james.chong@york.ac.uk.

[7] The abbreviations used are: MCM, minichromosome maintenance; hMCM, human MCM.

tionally modulated *in vivo* by phosphorylation, although this is not essential for replication elongation (16). The presence of inhibitory phosphorylations might explain why some purified MCM complexes produced in eukaryotic expression systems do not demonstrate significant helicase activity. Current methods for MCM2–7 complex analysis rely on purification from yeast or insect cells, potentially complicating the interpretation of results, as the purified MCM2–7 complexes may have been post-translationally modified prior to purification.

We report the development of a bacterial expression protocol that allows the production of a recombinant human MCM2–7 (hMCM) complex in *Escherichia coli*. Our hMCM complex exhibits DNA unwinding and ATP hydrolysis with a different salt sensitivity from that reported for the yeast complex (17). Structures of the protein obtained by EM methods show that hMCM forms an asymmetric hexameric complex that undergoes a conformational change in the presence of a forked DNA substrate that it is also capable of unwinding. The generation of recombinant hMCM represents the development of an important tool for understanding the mechanisms governing human DNA replication. This may ultimately improve our ability to manipulate cell proliferation and therefore design useful and specific cancer treatments.

EXPERIMENTAL PROCEDURES

Expression and Purification of the MCM2–7 Complex—PCR-amplified MCM2–7 cDNAs (see primers in Table 2) were cloned into Ek/LIC Duet vectors (Novagen). pET32-MCM2/7, pRSF-MCM3/5, and pCDF-MCM4/6 were transformed into *E. coli* Rosetta 2(DE3) cells (Novagen) and grown in a 75-liter fermenter. The hMCM complex was bound to HIS-Select cobalt affinity gel (Sigma) and passed over Superdex 200 gel filtration and Mono Q columns. Fractions containing MCM2–7 were pooled; dialyzed against 25 mM HEPES (pH 8.0), 200 mM sodium glutamate, 1 mM DTT, and 0.5 mM PMSF; flash-frozen in small aliquots; and stored at −80 °C. Site-directed mutagenesis of pET32-MCM2/7, pRSF-MCM3/5, and pCDF-MCM4/6 produced inactive point mutations in the Walker A motif for each hMCM subunit (MCM2(K529E), MCM3(K351E), MCM4(K516E), MCM5(K387E), MCM6(K402E), and MCM7(K387E)). ATPase-deficient mutant protein was produced and purified as described for the WT type protein.

Western Blotting—Individual MCM subunits were confirmed by Western blotting the purified protein using primary antibodies: anti-MCM2 (CS732) (18), anti-MCM3 (clone 3A2; Medical & Biological Laboratories), anti-MCM4 (G-7; Santa Cruz Biotechnology), anti-MCM5 (clone 33; BD Biosciences), anti-MCM6 (clone 1/MCM6; BD Biosciences), and anti-MCM7 (141.2; Santa Cruz Biotechnology).

ATPase Assays—Reactions were modified from Ref. 6 as follows. Reactions containing 30 mM K_2HPO_4/KH_2PO_4 buffer (pH 8.5), 1 mM DTT, 100 μg/ml BSA, 2% (v/v) glycerol, 10 mM magnesium acetate, 1.5 nmol of unlabeled ATP, 3.08 pmol of [α-^{32}P]ATP (800 Ci/mmol; ICN), 3.5 nM circular dsDNA (pUC119 unless stated otherwise), and 176 nM protein were assembled on ice.

DNA Helicase Substrate—Oligonucleotide HS2 (Table 2) was radiolabeled and annealed to oligonucleotide HS1 as described (6).

Helicase Assays—Helicase reactions (4 nM ^{32}P-labeled forked substrate, MCM2–7 as indicated, 30 mM K_2HPO_4/KH_2PO_4 buffer (pH 8.5), 300 mM potassium glutamate, 1 mM DTT, 100 μg/ml BSA, 2% (v/v) glycerol, 10 mM magnesium acetate, and 4 mM ATP) were incubated for 1 h at 37 °C and stopped using 0.25 volume of 80 mM EDTA, 0.8% (w/v) SDS, 40% (v/v) glycerol, 0.04% (w/v) xylene cyanol, and 0.04% (w/v) bromphenol blue. Reaction products were separated on Tris borate/EDTA-11%

TABLE 1

Comparison of *S. cerevisiae* and *H. sapiens* MCM amino acid insertions

aa, amino acids.

MCM	*S. cerevisiae* (aa)	*H. sapiens* (aa)	aa difference (*S. cerevisiae* − *H. sapiens*)	Insertion locations
2	868	904	−36 (−4%)	C
3	971	808	163 (20%)	N, C
4	933	863	70 (8%)	N
5	775	734	41 (6%)	N
6	1017	821	196 (24%)	N, C
7	845	719	126 (18%)	N

TABLE 2

List of oligonucleotides used in this study

Oligonucleotide	Sequence
MCM2	
Forward	gcgggcccggcctccatggcggaatcatcggaatccttcacc
Reverse	gaggagaagcccggtcagaactgctgcaggatcattttcc
MCM3	
Forward	gcgggcccggccttcatggcgggtaccgtggtgctggac
Reverse	gaggagaagcccggtcagatgaggaagatgatgccctcag
MCM4	
Forward	gcgggcccggccttcatgtcgtccccggcgtcgacccc
Reverse	gaggagaagcccggtcagagcaagcgcacggtcttccc
MCM5	
Forward	gacgacgacaagatgtcgggattcgacgatcctggc
Reverse	cgcgggcggccgtcacttgaggcggtagagaaccttgc
MCM6	
Forward	gacgacgacaagatggacctcgcggcggcagcgg
Reverse	cgcgggcggccgtcaatcttcgagcaagtagttaggg
MCM7	
Forward	gacgacgacaagatggcactgaaggactacgcgctag
Reverse	cgcgggcggccgtcagacaaaagtgatccgtgtccggg
HF150	cctggcgttacccaacttaatcgccttgcagcacatcccccttctttttttttttttttttttttttttttttttttttttttttttttttttttttttttttt
HR80	tttttttttttttttttttttttttttttttttttgaaagggggatgtgctgcaaggcgattaagttgggtaacgccagg
HS1	gggacgcgtcggcctggcacgtcggccgctgcggccaggcacccgatggcgtttgtttgtttgtttgtttgttt
HS2	tttgtttgtttgtttgtttgtttgtttgtttgccgacgtgccaggccgacgcgtccc

(w/v) polyacrylamide gels (2 h, 80 V). Gels were dried, imaged, and quantified using a Bio-Rad Molecular Imager FX and Quantity One software.

Binding of Duplex DNA to hMCM for EM—No-salt annealing buffer (200 mM HEPES (pH 8.0) and 5 mM EDTA) was added to 1 μM HF150 (150 bp) and 1 μM HR80 (80 bp) (Table 2). DNA was annealed at 95 °C for 3 min, followed by cooling at 0.02 °C/s to 23 °C. The temperature was kept at 23 °C for 1 min. hMCM (8 μg) was incubated with 60 nM duplex DNA in annealing buffer (50 mM HEPES (pH 7.5), 2 mM DTT, 50 μg/ml BSA, 10 mM magnesium acetate, and 4 mM ATP) for 60 min at 37 °C to bind hMCM and duplex DNA. Samples were snap-frozen in liquid nitrogen.

Electron Microscopy—hMCM samples were applied to continuous carbon grids and stained with freshly made methylamine tungstate (pH 7). Data were collected on an FEI T12 microscope at a magnification of ×67,000 and an accelerating voltage of 120 kV, recorded on Kodak SO-163 films, and digitized using a Zeiss Photoscan densitometer (14-μm scanning step, corresponding to 2.5 Å/pixel) before analysis.

Image Processing—Particle picking was carried out automatically using Boxer (EMAN suite (19)). Analysis of the contrast transfer function and correction was completed using CTFIT (EMAN suite (19)). Image analysis was performed with IMAGIC-5 (20). Images were normalized to the same S.D. and bandpass-filtered. The low-resolution cutoff was ~100 Å to remove uneven background in particle images, and the high-resolution cutoff was ~7 Å. Images were subjected to an alignment procedure, followed by statistical analysis. Alignment and classification of images were performed as described previously (20) and yielded classes representing characteristic views of the molecule. Primary structural analysis of hMCM and hMCM plus DNA complexes was performed using an *ab initio* approach in which the orientations of the best 10–15 image classes were determined by angular reconstitution using C1 startup. Three-dimensional maps were calculated using the exact filtered backprojection algorithm (20). Structural analysis was performed using several starting models with several different sets of image classes for *ab initio* reconstructions. The first reconstructions were used for the following rounds of alignment and classification of images. The structures of the complexes were refined by an iterative procedure with the number of classes gradually increased. The final reconstruction for hMCM alone was calculated from the best 100 classes containing ~11 images each. For hMCM plus DNA, the final reconstruction was calculated from the best 155 classes containing ~10 images each. Resolution of the map was assessed using the 0.5 threshold of Fourier shell correlation (21), which corresponds to 23 Å. Domain fitting into the three-dimensional map of hMCM and hMCM plus DNA complexes was performed manually with UCSF Chimera (22). Illustrations were generated using UCSF Chimera. Surface representations (unless stated otherwise) are displayed at a threshold level of 3σ (S.D. of densities within EM maps), which corresponds to ~100% of the expected mass at a specific protein density of 0.84 kDa/Å^3.

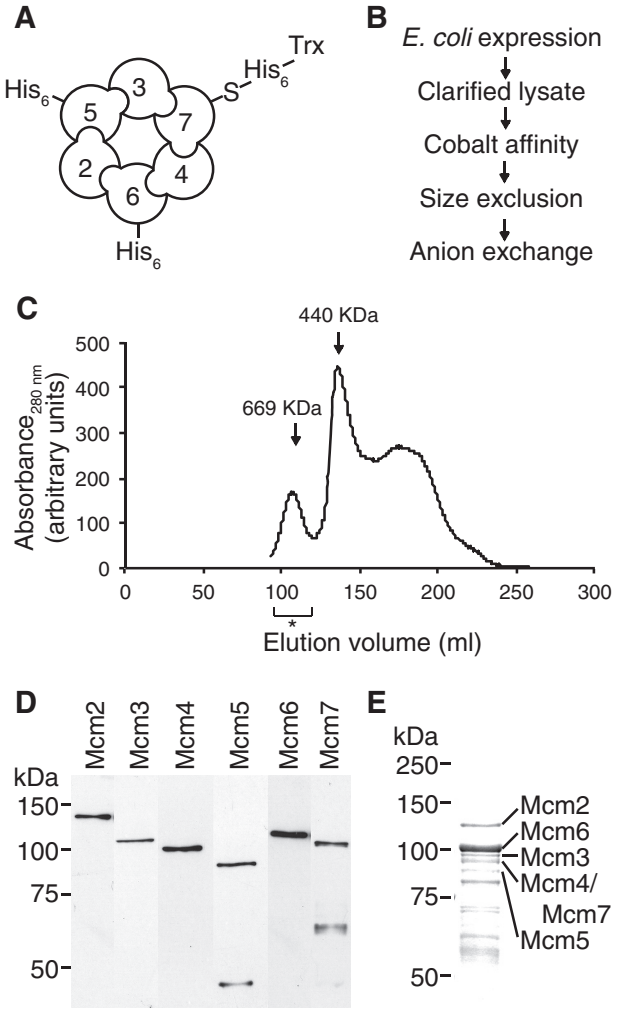

FIGURE 1. **Purification of a bacterially expressed hMCM complex.** *A*, schematic of the recombinant hMCM complex. Shown is the predicted arrangement of MCM2–7 subunits indicating which subunits have N-terminal affinity tags to aid in protein purification. *B*, purification scheme for the recombinant hMCM complex. *C*, gel filtration elution profile for the recombinant hMCM complex. The elution fractions pooled are indicated by the *asterisk*. The protein markers thyroglobulin (669 kDa) and ferritin (440 kDa) are shown. *D*, Western blot using antibodies specific to individual MCM subunits, showing all six hMCM subunits in the purified complex. *E*, the purified hMCM complex separated by 10% (w/v) SDS-PAGE and visualized by Coomassie Blue staining.

RESULTS

Production of a Soluble hMCM Complex—To avoid potential activity-inhibiting phosphorylation by kinases present in eukaryotic expression systems, we coexpressed the hMCM2–7 proteins as a stable soluble complex in *E. coli* (Fig. 1*A*). The complex was purified according to the scheme outlined in Fig. 1*B*. The gel filtration elution profile for hMCM shows that the peak purified is at ~600 kDa (Fig. 1*C*). The presence of all six hMCM subunits in the purified complex was demonstrated by Western blotting using specific antibodies (Fig. 1*D*). Consistent with our Western blot results, visualization of the complex using Coomassie Blue-stained SDS-polyacrylamide gel revealed the presence of some degradation products (confirmed by MS analysis) in addition to all six full-length hMCM subunits (Fig. 1*E*). The MCM6 band is more intense than the bands of the other subunits in the Coomassie Blue gel (Fig. 1*E*), which could be due to differential staining based on protein

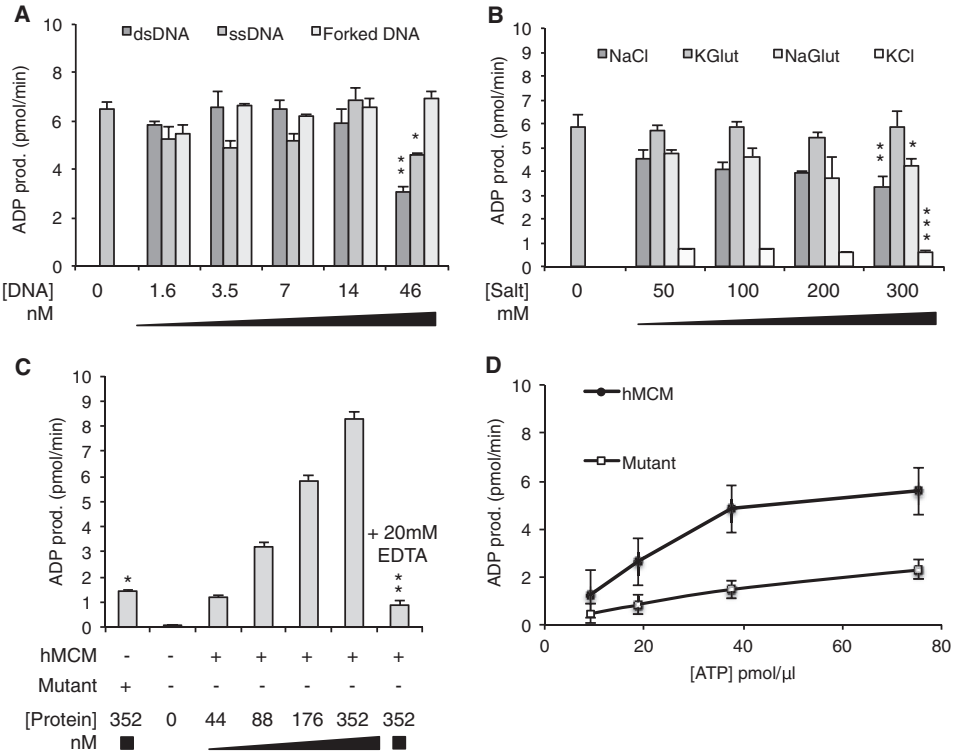

FIGURE 2. **WT hMCM possesses ATPase activity.** *A*, 46 nM closed circular ssDNA (hMCM hexamer/DNA molar ratio of 3.8:1) reduced ATP hydrolysis by one-third, and closed circular dsDNA reduced ATP hydrolysis by ~50%. Forked DNA had little overall effect. Statistics compare the *labeled bars* with 0 nM DNA. *, $p = 0.022$; **, $p = 0.0019$. *B*, potassium glutamate (*KGlut*) had no effect on ATPase activity in the presence of 3.5 nM dsDNA. Increasing the concentrations of NaCl and sodium glutamate (*NaGlut*) reduced ATP hydrolysis, and the addition of KCl greatly reduced ATP hydrolysis. Statistics compare *labeled bars* with 0 mM salt. *, $p = 0.018$; **, $p = 0.013$; ***, $p = 0.00027$. *C*, ATPase activity increases with protein concentration in the presence of 3.5 nM dsDNA and is inhibited by the addition of 20 mM EDTA to chelate the Mg^{2+}. ATPase-deficient mutant hMCM showed 6-fold lower ATP hydrolysis activity compared with WT hMCM. Statistics compare *labeled bars* with 352 nM hMCM. *, $p = 0.0015$; **, $p = 0.00014$. *D*, rate of ATP hydrolysis by WT hMCM and ATPase-deficient mutant hMCM in molecules of ADP released per min with optimized conditions (3.5 nM dsDNA, 300 mM potassium glutamate, and 176 nM hMCM). The maximum rate of ATP hydrolysis was 16.7 pmol of ADP produced (*prod.*) per min/pmol of WT hMCM and 3.9 pmol of ADP produced per min/pmol of mutant hMCM in the presence of 3.5 nM dsDNA. The data in *A–C* are mean values of three replicates, and the data in *D* are mean values of two assays. *Error bars* show S.D.

composition or a slight excess of uncomplexed MCM6 being present in the soluble fraction after expression in *E. coli*. Typically, we produce 82.5 μg of hMCM/liter of *E. coli* culture. A complex harboring inactivating point mutations in the Walker A motifs of each hMCM subunit (MCM2(K529E), Mcm3-(K351E), MCM4(K516E), MCM5(K387E), MCM6(K402E), and MCM7(K387E)) was produced in the same way.

ATP Hydrolysis Activity of hMCM—The purified WT hMCM complex and ATPase-deficient mutant complexes were tested for their ability to hydrolyze ATP in the presence and absence of a series of DNA substrates (at hMCM hexamer/DNA molar ratios ranging from 110:1 to 3.8:1) (Fig. 2*A*). hMCM exhibited ATP hydrolysis, which was not increased by the addition of DNA. High concentrations (46 nM) of closed circular dsDNA inhibited ATP hydrolysis by ~50% compared with lower concentrations of dsDNA, possibly due to a substrate competition effect preventing the MCM proteins from forming a productive complex. A similar but smaller effect was observed for closed circular ssDNA. A forked DNA substrate had a negligible effect on hydrolysis activity at the concentrations tested. Subsequent ATP hydrolysis assays were carried out in the presence of 3.5 nM dsDNA.

On the basis of previous reports of specific salt requirements for yeast MCM activity *in vitro* (17), we examined the ability of hMCM to hydrolyze ATP in the presence of sodium chloride, sodium glutamate, potassium chloride, and potassium glutamate (Fig. 2*B*). Increased sodium chloride concentrations resulted in a statistically significant decrease in ATP hydrolysis. A similar effect was observed for sodium glutamate. The addition of 50 mM potassium chloride resulted in a pronounced inhibition of ATPase activity. Strikingly, the presence of 300 mM potassium glutamate, twice the physiological salt concentration, had no effect on ATPase activity (Fig. 2*B*). As expected, increasing concentrations of hMCM resulted in increased ATP hydrolysis (Fig. 2*C*). The addition of 20 mM EDTA significantly reduced ATP hydrolysis by hMCM, as did replacing the WT protein with the ATPase-deficient mutant complex (Fig. 2*C*), as expected from previous studies in *S. cerevisiae* (5, 23). Using the optimum assay conditions identified (3.5 nM dsDNA, 300 mM potassium glutamate, and 176 nM hMCM), we measured the rate of ATP hydrolysis for WT and mutant hMCM (Fig. 2*D*). The maximum rate of ATP hydrolysis was 16.7 pmol of ADP released per min/pmol of WT hMCM compared with 3.9 pmol of ADP released per min/pmol of mutant hMCM.

ATP-dependent DNA Unwinding by hMCM—We tested our purified recombinant hMCM complexes for DNA helicase activity using a forked DNA substrate in the presence or absence of ATP. WT hMCM exhibited a protein concentration- and ATP-dependent DNA unwinding activity (Fig. 3). With WT hMCM, we observed 38 and 50% displacement by

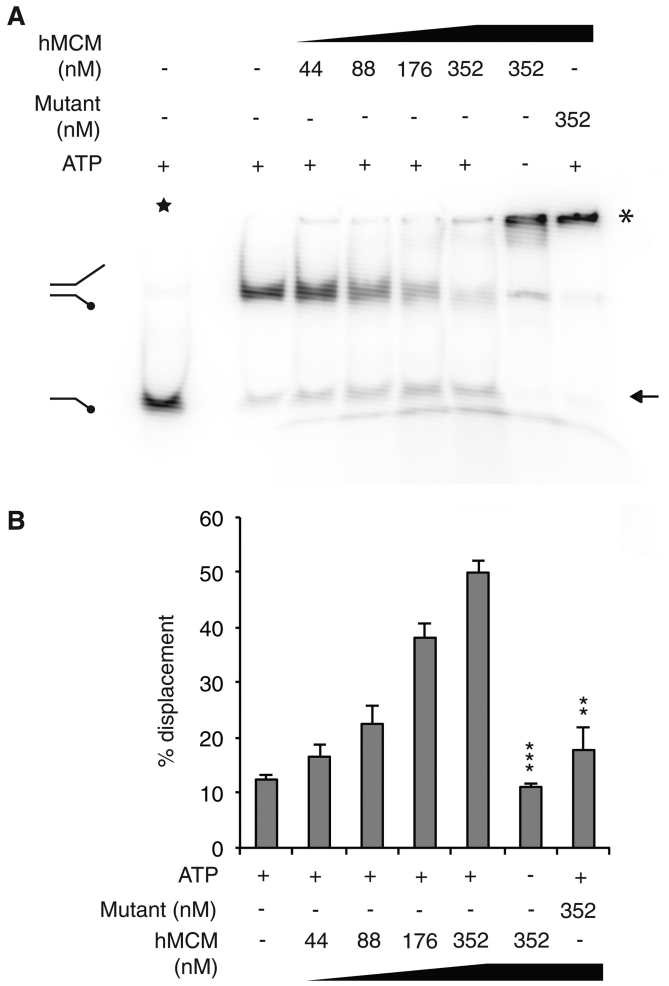

FIGURE 3. **Recombinant hMCM displays DNA helicase activity.** *A*, a forked DNA substrate was incubated with increasing concentrations of hMCM in the absence or presence of ATP. Heat-denatured boiled substrate (⋆) and no-protein lanes were included as controls. The *arrow* indicates the position of displaced substrate, and the *asterisk* indicates substrate with unusual mobility, perhaps indicating that hMCM that is bound to DNA. *B*, the amount of single-stranded substrate in each reaction was quantified as a percentage of the boiled substrate control. The data shown are mean values for four independent assays, an example of which is shown in *A*. *Error bars* indicate S.E. Statistics compare *labeled lanes* with 352 nM hMCM plus ATP. ***, $p = 0.00013$; **, $p = 0.0014$.

176 M and 352 nM hMCM2–7, respectively (Fig. 3), broadly comparable with the reported 52% displacement by 110 nM yeast Mcm2–7 (17). Under conditions in which ATP could not be hydrolyzed, *i.e.* either WT hMCM in the absence of ATP or mutant hMCM in the presence of ATP, helicase activity was substantially reduced (Fig. 3*B*), consistent with ATP hydrolysis being required for helicase activity.

EM Structure of Recombinant hMCM—The structures of the purified hMCM complex alone and bound to forked DNA were obtained by EM of negatively stained particles. Structures were obtained using a single-particle approach with C1 symmetry (Fig. 4). Our results reveal that the complex forms ring-shaped hexamers with a diameter of 145 Å and a height of 120 Å (Fig. 4*C*). Our asymmetric reconstructions (Fig. 4) clearly show that the complexes contain six subunits. However, the resolution does not allow us to identify the position of each subunit. When observed in the presence of forked DNA (Fig. 4*C*, *lower row*), the hMCM structure has a different conformation, with a more defined two-tiered hexameric shape and a more obviously open central cavity. The atomic model of the hexamer of *Sulfolobus solfataricus* MCM (Protein Data Bank ID 3F9V) fits neatly into our reconstruction (Fig. 5).

DISCUSSION

ATP hydrolysis has been demonstrated for MCM complexes derived from archaea (5) and eukaryotes (23, 24). We found that the addition of DNA did not stimulate ATP hydrolysis by purified hMCM. This is consistent with reports of *S. cerevisiae* Mcm2–7, in which DNA did not stimulate ATP hydrolysis (23, 25). It is worth noting that this is in contrast to the Mcm4-Mcm6-Mcm7 subcomplex, which is stimulated by DNA (26, 27). In agreement with observations from archaeal MCM proteins (5), high concentrations of dsDNA were in fact inhibitory. With respect to salt sensitivity, 50 mM potassium chloride strongly inhibited the ATPase activity of hMCM, whereas potassium glutamate, even at a concentration of 300 mM, had no such effect. These findings are consistent with results reported for the DNA helicase activity of *S. cerevisiae* MCM (17).

Binding and hydrolysis of ATP by MCM purified from *S. cerevisiae* have recently been shown to be required for Cdt1 release and double-hexamer formation (28), with the ATPase sites of different MCM subunits implicated in different stages of MCM loading and activation (29). The interface between subunits 2 and 5 of the *S. cerevisiae* Mcm2–7 complex is thought to function as an ATP-dependent "gate," the opening of which enables the toroidal complex to be loaded onto topologically closed DNA (17). The recombinant hMCM complex produced here is an important tool to analyze the loading and activation of the human complex in light of this finding.

Robust ATP-dependent DNA helicase activities were first demonstrated using archaeal homohexamers (5). Limited DNA helicase activity was originally demonstrated for a hexameric complex purified from HeLa cells that contained hMCM subunits 4, 6, and 7, probably as a dimer of trimers (24). This activity was inhibited by the addition of mouse MCM2 (30). The salt-sensitive DNA helicase activity of a heterohexameric Mcm2–7 complex was first demonstrated using *S. cerevisiae* proteins purified after baculovirus expression (17), and DNA unwinding activity of higher eukaryotic MCM complexes has been observed with the Cdc45-MCM-GINS complex from *Drosophila* (15). Here, we described the first demonstration of helicase activity for the hMCM2–7 complex.

Our results show that ATP hydrolysis is a requirement for DNA helicase activity. The negligible unwinding and ATPase activities in the mutant hMCM assays suggest that the mutant and WT protein preparations were both free from contaminating *E. coli* helicases/ATPases. Under ATPase null conditions (either no ATP or mutant hMCM), a large proportion of the helicase substrate migrated more slowly on native polyacrylamide gel. Similar mobility shift effects were observed previously for the *Methanothermobacter thermautotrophicus* MCM complex when samples were incubated on ice (6). This suggests that the hMCM protein binds to the substrate in the absence of ATP (or ATP hydrolysis) but cannot unwind it. This is consis-

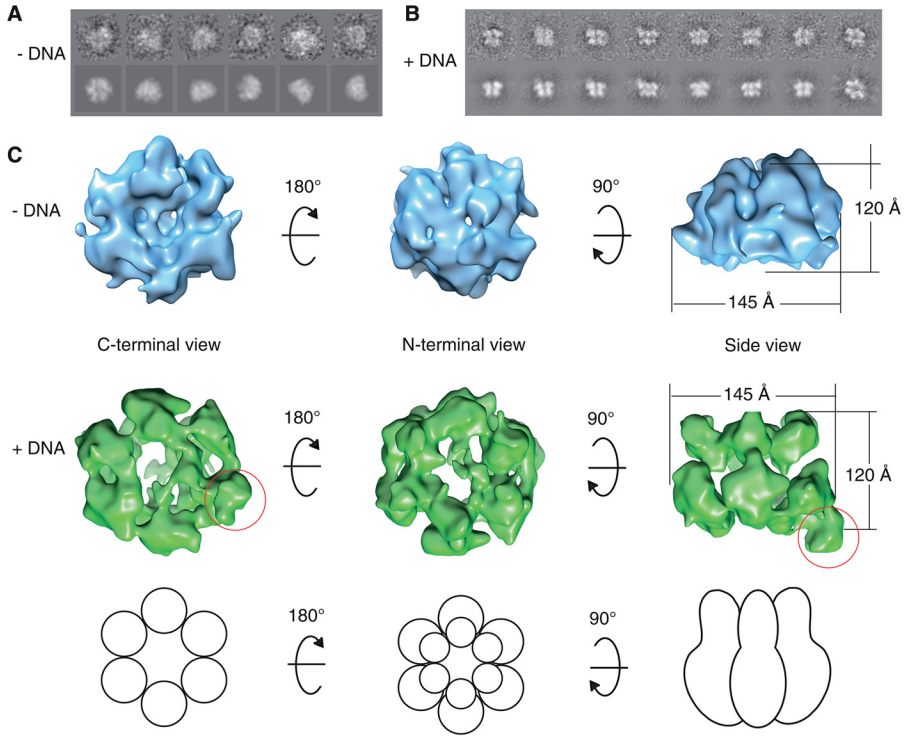

FIGURE 4. *A*, hMCM classes and reprojections used in the final reconstruction for hMCM alone. *B*, same as in *A* for hMCM plus DNA. *C*, negative stain, single-particle asymmetric EM three-dimensional reconstruction of hMCM to 23 Å resolution. *Upper row*, hMCM alone (*blue*) from three different aspects. The complex undergoes a conformational change when hMCM is bound to forked DNA (*middle row*, *green*). The *red circle* highlights protrusion thought to be DNA binding to hMCM. Sizes are indicated in angstroms. *Lower row*, schematic representation of hMCM subunit configuration.

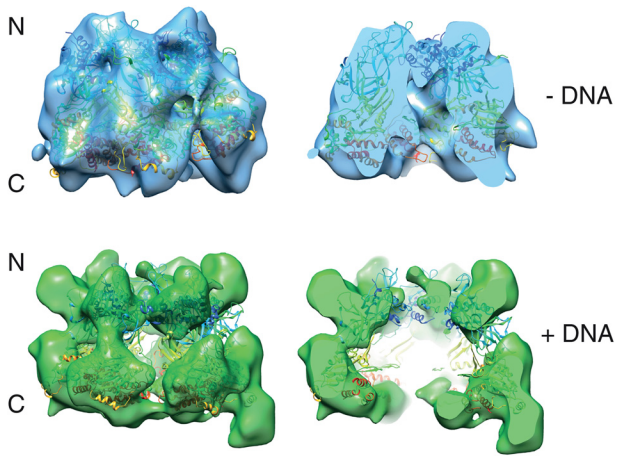

FIGURE 5. **The crystal structure of *S. solfataricus* MCM fits into our reconstructions.** Shown is hMCM alone (*blue*) and bound to forked DNA (*green*) fitted with the nearly full-length *S. solfataricus* MCM crystal structure (Protein Data Bank ID 3F9V) (8). The full-length hMCM structure (*left*) and a slice through hMCM (*right*) show a central cavity in both reconstructions.

tent with the idea that ATP hydrolysis is not required for DNA-protein interactions but is required for DNA unwinding (31).

Overall, these results indicate that the recombinant hMCM complex exhibits DNA helicase activity and that post-translational modifications to hMCM or accessory proteins such as Cdc45 and GINS are not required for the unwinding of naked DNA. The presence of Cdc45 and GINS may be required only for remodeling or unwinding DNA packaged into chromatin.

The size and shape of our hMCM complex are consistent with the organization of oligomeric complexes reported for MCM from other eukaryotes (32, 33). Analysis of a population of *Drosophila* Mcm2–7 complexes revealed that they exist in two different states: a planar notched ring and an open spiral shape (32). Reconstructions of Mcm2–7 from *Encephalitozoon cuniculi* suggest that this Mcm2–7 complex is naturally found in the open spiral shape (34). Our reconstruction of the human complex is more similar to the notched ring, similar to *S. cerevisiae* (35), but this does not preclude the existence of a minority of spiral-shaped complexes in our sample.

Interestingly, the conformation taken by hMCM in the presence of DNA is somewhat similar to that which has been reported for *S. cerevisiae* Mcm2–7 in the absence of DNA (36). One possible reason for the differences observed between the yeast and human proteins in the absence of DNA could be the differences in their primary sequences (outlined in Table 1). The prominent projection that appears on the C-terminal surface of one of the hMCM subunits in the presence of DNA (Fig. 4*C*, *red circle*) could be either the bound 45-bp double-stranded portion of the DNA substrate (as ssDNA is too small to be clearly visualized at this resolution) or a protein domain displaced by the presence of the DNA, such as a flexible C-terminal domain. Further work is required to determine which hMCM subunit binds DNA under these conditions.

hMCM is an important factor in cell proliferation and therefore, by extension, cancer development. The ability to produce significant quantities of hMCM for analysis is an important step forward. Our biochemical findings show that the recombinant complex is active *in vitro*, and our structural studies show that its conformation is altered when bound to DNA. Our system enables the targeted manipulation of individual proteins within the hMCM complex, providing the potential to address in detail

the important differences between individual subunits in the hMCM heterohexamer. It also provides the potential to develop screens for clinically relevant hMCM inhibitors.

Acknowledgments—We thanks Christoph Baumann and Peter McGlynn for comments on the manuscript. cDNA clones of hMCM proteins and polyclonal antibody CS732 were gifts from J. Méndez (Centro Nacional de Investigaciones Oncológicas).

REFERENCES

1. Byers, B., and Goetsch, L. (1975) Behavior of spindles and spindle plaques in cell-cycle and conjugation of *Saccharomyces-cerevisiae*. *J. Bacteriol.* **124,** 511–523
2. Kim, J. H., Na, C. Y., Choi, S. Y., Kim, H. W., Du Kim, Y., Kwon, J. B., Chung, M. Y., Hong, J. M., and Park, C. B. (2010) Integration of gene-expression profiles and pathway analysis in ascending thoracic aortic aneurysms. *Ann. Vasc. Surg.* **24,** 538–549
3. Munkley, J., Copeland, N. A., Moignard, V., Knight, J. R., Greaves, E., Ramsbottom, S. A., Pownall, M. E., Southgate, J., Ainscough, J. F., and Coverley, D. (2011) Cyclin E is recruited to the nuclear matrix during differentiation, but is not recruited in cancer cells. *Nucleic Acid. Res.* **39,** 2671–2677
4. Tye, B. K. (1999) MCM proteins in DNA replication. *Annu. Rev. Biochem.* **68,** 649–686
5. Chong, J. P., Hayashi, M. K., Simon, M. N., Xu, R. M., and Stillman, B. (2000) A double-hexamer archaeal minichromosome maintenance protein is an ATP-dependent DNA helicase. *Proc. Natl. Acad. Sci. U.S.A.* **97,** 1530–1535
6. Jenkinson, E. R., and Chong, J. P. (2006) Minichromosome maintenance helicase activity is controlled by N- and C-terminal motifs and requires the ATPase domain helix-2 insert. *Proc. Natl. Acad. Sci. U.S.A.* **103,** 7613–7618
7. Fletcher, R. J., Bishop, B. E., Leon, R. P., Sclafani, R. A., Ogata, C. M., and Chen, X. S. (2003) The structure and function of MCM from archaeal *M. thermoautotrophicum*. *Nat. Struct. Biol.* **10,** 160–167
8. Brewster, A. S., Wang, G., Yu, X., Greenleaf, W. B., Carazo, J. M., Tjajadi, M., Klein, M. G., and Chen, X. S. (2008) Crystal structure of a near-full-length archaeal MCM: functional insights for an AAA plus hexameric helicase. *Proc. Natl. Acad. Sci. U.S.A.* **105,** 20191–20196
9. Stead, B. E., Brandl, C. J., and Davey, M. J. (2011) Phosphorylation of Mcm2 modulates Mcm2–7 activity and affects the cell's response to DNA damage. *Nucleic Acids Res.* **39,** 6998–7008
10. Ibarra, A., Schwob, E., and Méndez, J. (2008) Excess MCM proteins protect human cells from replicative stress by licensing backup origins of replication. *Proc. Natl. Acad. Sci. U.S.A.* **105,** 8956–8961
11. Snyder, M., He, W., and Zhang, J. J. (2005) The DNA replication factor MCM5 is essential for Stat1-mediated transcriptional activation. *Proc. Natl. Acad. Sci. U.S.A.* **102,** 14539–14544
12. Groth, A., Corpet, A., Cook, A. J., Roche, D., Bartek, J., Lukas, J., and Almouzni, G. (2007) Regulation of replication fork progression through histone supply and demand. *Science* **318,** 1928–1931
13. Chong, J. P., Mahbubani, H. M., Khoo, C. Y., and Blow, J. J. (1995) Purification of an MCM-containing complex as a component of the replication licensing system. *Nature* **375,** 418–421
14. Tada, S., Li, A., Maiorano, D., Méchali, M., and Blow, J. J. (2001) Repression of origin assembly in metaphase depends on inhibition of RLF-B/Cdt1 by geminin. *Nat. Cell Biol.* **3,** 107–113
15. Moyer, S. E., Lewis, P. W., and Botchan, M. R. (2006) Isolation of the Cdc45/Mcm2–7/GINS (CMG) complex, a candidate for the eukaryotic DNA replication fork helicase. *Proc. Natl. Acad. Sci. U.S.A.* **103,** 10236–10241
16. Poh, W. T., Chadha, G. S., Gillespie, P. J., Kaldis, P., and Blow, J. J. (2014) *Xenopus* Cdc7 executes its essential function early in S phase and is counteracted by checkpoint-regulated protein phosphatase 1. *Open Biol.* **4,** 130138
17. Bochman, M. L., and Schwacha, A. (2008) The MCM2–7 complex has *in vitro* helicase activity. *Mol. Cell* **31,** 287–293
18. Ekholm-Reed, S., Méndez, J., Tedesco, D., Zetterberg, A., Stillman, B., and Reed, S. I. (2004) Deregulation of cyclin E in human cells interferes with prereplication complex assembly. *J. Cell Biol.* **165,** 789–800
19. Tang, G., Peng, L., Baldwin, P. R., Mann, D. S., Jiang, W., Rees, I., and Ludtke, S. J. (2007) EMAN2: an extensible image processing suite for electron microscopy. *J. Struct. Biol.* **157,** 38–46
20. van Heel, M., Harauz, G., Orlova, E. V., Schmidt, R., and Schatz, M. (1996) A new generation of the IMAGIC image processing system. *J. Struct. Biol.* **116,** 17–24
21. van Heel, M., Gowen, B., Matadeen, R., Orlova, E. V., Finn, R., Pape, T., Cohen, D., Stark, H., Schmidt, R., Schatz, M., and Patwardhan, A. (2000) Single-particle electron cryo-microscopy: towards atomic resolution. *Q. Rev. Biophys.* **33,** 307–369
22. Goddard, T. D., Huang, C. C., and Ferrin, T. E. (2007) Visualizing density maps with UCSF Chimera. *J. Struct. Biol.* **157,** 281–287
23. Schwacha, A., and Bell, S. P. (2001) Interactions between two catalytically distinct MCM subgroups are essential for coordinated ATP hydrolysis and DNA replication. *Mol. Cell* **8,** 1093–1104
24. Ishimi, Y. (1997) A DNA helicase activity is associated with an MCM4, -6, and -7 protein complex. *J. Biol. Chem.* **272,** 24508–24513
25. Bochman, M. L., Bell, S. P., and Schwacha, A. (2008) Subunit organization of Mcm2–7 and the unequal role of active sites in ATP hydrolysis and viability. *Mol. Cell. Biol.* **28,** 5865–5873
26. Biswas-Fiss, E. E., Khopde, S. M., and Biswas, S. B. (2005) The Mcm467 complex of *Saccharomyces cerevisiae* is preferentially activated by autonomously replicating DNA sequences. *Biochemistry* **44,** 2916–2925
27. You, Z., Ishimi, Y., Mizuno, T., Sugasawa, K., Hanaoka, F., and Masai, H. (2003) Thymine-rich single-stranded DNA activates Mcm4/6/7 helicase on Y-fork and bubble-like substrates. *EMBO J.* **22,** 6148–6160
28. Coster, G., Frigola, J., Beuron, F., Morris, E. P., and Diffley, J. F. (2014) Origin licensing requires ATP binding and hydrolysis by the MCM replicative helicase. *Mol. Cell* **55,** 666–677
29. Kang, S., Warner, M. D., and Bell, S. P. (2014) Multiple functions for Mcm2–7 ATPase motifs during replication initiation. *Mol. Cell* **55,** 655–665
30. Ishimi, Y., Komamura, Y., You, Z., and Kimura, H. (1998) Biochemical function of mouse minichromosome maintenance 2 protein. *J. Biol. Chem.* **273,** 8369–8375
31. McGeoch, A. T., Trakselis, M. A., Laskey, R. A., and Bell, S. D. (2005) Organization of the archaeal MCM complex on DNA and implications for the helicase mechanism. *Nat. Struct. Mol. Biol.* **12,** 756–762
32. Costa, A., Ilves, I., Tamberg, N., Petojevic, T., Nogales, E., Botchan, M. R., and Berger, J. M. (2011) The structural basis for MCM2–7 helicase activation by GINS and Cdc45. *Nat. Struct. Mol. Biol* **18,** 471–477
33. Remus, D., Beuron, F., Tolun, G., Griffith, J. D., Morris, E. P., and Diffley, J. F. (2009) Concerted loading of MCM2–7 double hexamers around DNA during DNA replication origin licensing. *Cell* **139,** 719–730
34. Lyubimov, A. Y., Costa, A., Bleichert, F., Botchan, M. R., and Berger, J. M. (2012) ATP-dependent conformational dynamics underlie the functional asymmetry of the replicative helicase from a minimalist eukaryote. *Proc. Natl. Acad. Sci. U.S.A.* **109,** 11999–12004
35. Samel, S. A., Fernández-Cid, A., Sun, J., Riera, A., Tognetti, S., Herrera, M. C., Li, H., and Speck, C. (2014) A unique DNA entry gate serves for regulated loading of the eukaryotic replicative helicase MCM2–7 onto DNA. *Genes Dev.* **28,** 1653–1666
36. Evrin, C., Clarke, P., Zech, J., Lurz, R., Sun, J., Uhle, S., Li, H., Stillman, B., and Speck, C. (2009) A double-hexameric MCM2–7 complex is loaded onto origin DNA during licensing of eukaryotic DNA replication. *Proc. Natl. Acad. Sci. U.S.A.* **106,** 20240–20245